IOP Publishing New J. Phys. 26 (2024) 033052 https://doi.org/10.1088/1367-2630/ad3573

New Journal of Physics
The open access journal at the forefront of physics

Deutsche Physikalische Gesellschaft DPG
IOP Institute of Physics

Published in partnership with: Deutsche Physikalische Gesellschaft and the Institute of Physics

OPEN ACCESS

RECEIVED
27 September 2023

REVISED
9 March 2024

ACCEPTED FOR PUBLICATION
19 March 2024

PUBLISHED
2 April 2024

PAPER

Manipulation and enhancement of the performance of Otto cycle in the presence of nonthermal reservoirs

Rui Huang, Yun-Jie Xia and Zhong-Xiao Man*

School of Physics and Physical Engineering, Shandong Provincial Key Laboratory of Laser Polarization and Information Technology, Qufu Normal University, 273165 Qufu, People's Republic of China

* Author to whom any correspondence should be addressed.

E-mail: manzhongxiao@163.com

Keywords: quantum thermodynamics, quantum coherence, Otto cycle, nonthermal reservoir

Abstract

In this work, we investigate the impact of energetic coherence in nonthermal reservoirs on the performance of the Otto cycle. We first focus on the situation where the working substance is a qubit. Due to the existence of coherence of nonthermal reservoir, various anomalous operating regimes such as the engine and refrigerator with efficiencies exceeding Carnot limits, as well as the hybrid refrigerator that can simultaneously achieve cooling and supplying work to an external agent, can occur. We demonstrate that the energetic coherence of the system's steady state plays a significant role in determining the cycle's functions by adding an additional stroke implementing dephasing and phase modulation operations in the cycle. The energetic coherence of the system is necessary to trigger the reservoir's coherence to exert influences on the cycle. We decompose the thermodynamic quantities to the components arising from the populations and coherence of the system, and find that the reservoir's coherence impacts the cycle from two aspects: one is the modification of the system's steady-state populations or temperatures, and the other is the direct contributions to the heat in the interaction between the system and reservoirs. We then explore the scenario where the working substance is two identical qubits, and the reservoirs are common to them. We show that the degenerate coherence of the system in the steady state can enhance the performances of the cycle as different machines. Additionally, the energetic coherence of the reservoir modifies the functions of the cycle still through the energetic coherence of the system rather than their degenerate coherence.

1. Introduction

Quantum resources, such as quantum coherence and correlations, have been widely applied in the quantum information technology achieving various tasks that would be impossible with the classical counterparts [1]. In this context, there is a natural expectation to extend the advantages of quantum features to other areas. Quantum thermodynamics (QT) exploits open quantum systems as working substances with the aim of discovering new thermodynamic characteristics in the quantum domains and improving thermodynamic tasks, among others. Therefore whether the advantages brought by genuine quantum effects can be found in QT has become a hot topic, although has long been debated [2–7]. One of the main ways to demonstrate quantum advantages in QT is to apply quantum coherence and correlations to the working substance of quantum thermal machines [8–25]. It was shown that small autonomous quantum refrigerators consisting of three qubits can achieve better cooling capacity and energy transport than classical refrigerators by utilizing entanglement of the qubits [8]. Quantum engines that use two coupled qubits to perform a generalized Otto cycle are found to have a like between generated work and the qubits' correlations caused by nonequilibrium common environments [9]. Quantum coherence sometimes inhibits the performance of quantum engines, similar to friction [10–12], which can be overcome and then be transformed into a quantum lubricant by adjusting the engine's parameters [13]. Experimental evidence confirms the advantage of quantum resources

in driving quantum engines, including the use of an ensemble of nitrogen vacancy centers in diamond [14] in the limit of small action [15] and a spin-1/2 system utilizing nuclear magnetic resonance techniques [16].

To influence quantum heat machines, quantum coherence and correlations can be applied directly in the working substance [8–25] or put into the reservoir to form a nonthermal reservoir. This perspective has been extensively studied [26–40] since the pioneering work by Scully *et al*, which showed that by virtue of nonthermal reservoir with coherence, the efficiency of a photonic Carnot engine can be increased to surpass the limit imposed by the thermal reservoir [41]. In this case, the coherence or correlations can be deemed as thermodynamic resources, or alternatively, a type of fuel being able to power the machines [26–28]. It was shown that the coherence in reservoirs may modify the functions of machines, in particular resulting in operating regimes that are classically forbidden, and enhance the performance of machines with efficiencies exceeding the Carnot bound [29, 30]. The correlations across two reservoirs, if taken as free resources, can enable the machine working between them exhibit different functions that might be inconsistent with thermodynamics laws [40]. The consistence can be recovered when energy exchanges in the preparation process of the nonthermal reservoir are involved [40]. For two interacting systems, where each is in contact with a nonthermal reservoir, it is possible to reverse the heat flow from the cold reservoir to the hot one by adjusting the relative phase of the coherent states of the two reservoirs [36]. This suggests that there are still unknown mechanisms at play in nonthermal reservoirs and further exploration is needed to better understand the abilities of nonthermal reservoirs. In fact, not all nonthermal environments can cause unconventional results, and certain conditions should be met for them to achieve those unusual effects [42].

The appropriate use of coherence in QT should take into account the types of coherences and whether to apply coherence in the system or in the environment. In [27, 37], coherences are classified into three types, namely, heat-exchange coherence, displacement coherence, and squeezing coherence. The heat-exchange coherence connects states of the same energy, also known as degenerate coherence. The displacement and squeezing coherences are both energetic coherences that are generated from the energy levels connected by transitions of one and two numbers of excitation, respectively. The nonthermal reservoir with degenerate coherence can still be considered an effective thermal reservoir with a modified temperature [26, 27, 43], while resembling a coherent drive (squeezed reservoir) with the displacement (squeezing) coherence [26, 27]. Energetic coherence in the system (working substance) can have a positive contribution to entropy production in the thermodynamic process [44], and improve machine performance by enabling it to operate in otherwise forbidden regimes [29, 30]. On the other hand, degenerate coherence can achieve a negative contribution to entropy production [45], induce heat flow reversals [46], and promote the heat current at no cost of dissipation [47]. Degenerate coherence is usually produced by collective interactions between multiple systems with a common reservoir [48].

Although various effects of coherence on quantum heat machines have been recognized, little exploration has been done on how the energetic coherence of nonthermal reservoir influence and enhance the performance of these machines. Understanding the mechanisms by which energetic coherence affects machines is crucial for taking advantage of quantum resources to design and enhance them. To shed light on this question, in this work, we study a modified Otto cycle [49–57] that features nonthermal reservoirs with energetic coherence and an additional stroke implementing dephasing and phase modulation operations on the system. We first consider a qubit as working substance of the Otto cycle. The existence of coherence in nonthermal reservoir lead the cycle to take on different operating regimes, in particular the otherwise forbidden one. These functions can be modified by either introducing the dephasing operation on the system's steady state or varying the phases therein. This provides not only an efficient method of achieving a machine with desired functions but also insight into the influential mechanism of energetic coherence in the reservoirs on the Otto cycle. It is found that the energetic coherences of both the reservoir and the system are jointly coupled to the system's populations, which in turn affect the energy exchanges between them and eventually the operating regimes of the cycle. The system's energetic coherence is thus necessary to trigger the nonthermal reservoir to produce a marked effect. We further address this point by decomposing the thermodynamic quantities into contributions from populations and coherences, identifying which component is responsible for the unconventional functions of the cycle. We then consider two identical qubits as the working substance. In this scenario, the degenerate coherence of the system can be yielded due to interactions with the common reservoir. We note that the system's degenerate coherence can enhance the performance of different machines even when both reservoirs are thermal. The energetic coherence of nonthermal reservoir imposes impact on the cycle still through the energetic coherence rather than the degenerate coherence of the system's steady state.

The continuous modes reservoir is obviously not suitable for injecting coherence or studying the associated effects on QT. To accomplish this, we adopt quantum collision model [58–66], which describes the reservoir as a group of identical particles, called ancillas, that interact with the system one after the other. The ancilla is usually modeled as a finite-sized quantum system, such as a qubit, making it easy to impose

coherence. The colliding ancilla is discarded after each interaction with the system to ensure Markovian dynamics. Due to its versatility and visual mechanism, the collision mode has been widely used in exploring QT [48, 67–76].

The paper is organized as follows. We begin by describing the modified Otto cycle in section 2. Next, in section 3, we focus on the case where a single qubit is the working substance, and only one reservoir is in the nonthermal state. Specifically, we set the cold reservoir to a nonthermal state in section 3.1 and the hot reservoir to a nonthermal state in section 3.2. In the section 3.3, we decompose thermodynamic quantities to identify which component, either the populations or coherence, is responsible for the unconventional functions of the cycle. In section 4, we extend our analysis by considering two qubits as the working substance. We demonstrate the enhancements of the machines by degenerate coherence when both reservoirs are in thermal states. We also show that the energetic coherence of a nonthermal reservoir still impacts the cycle through energetic coherence rather than the degenerate coherence of the system. The conclusion is made in section 5.

2. Otto cycle in the nonthermal reservoirs

The usual quantum Otto cycle consists of four processes that involve two isochoric processes where the system exchanges heat with hot and cold reservoirs, respectively, and two adiabatic processes where the system exchanges work with an external agent. In our model, we are not only interested in the effects of coherence of nonthermal reservoir but also in the role of the system's steady-state coherence and its synergies with reservoir's coherence in the cycle's performances. To achieve this, we introduce dephasing and phase modulation operations that act on the system before it interacts with the cold reservoir. As a result, our Otto cycle comprises five strokes, namely: (I) adiabatic compression, (II) contact with the hot reservoir, (III) adiabatic expansion, (IV) dephasing and phase modulation, and (V) contact with the cold reservoir.

To achieve work strokes, we change the Hamiltonian of the system $\hat{H}_S^i$ by controlling an external parameter, which in our model, is the frequency ω_i $(i = h, c)$. This frequency switches between ω_h and ω_c depending on whether the system is in contact with the hot or cold reservoirs R_h and R_c respectively. On the other hand, to achieve heat strokes, we alternate the system's contact between R_h and R_c. In the conventional Otto cycle, it is assumed that the two reservoirs are thermal and have inverse temperatures $\beta_i = 1/T_i$. We set $\hbar = k_B = 1$ here and hereafter. In contrast, our focus in this work is on the impact of the coherence of nonthermal reservoir on the performance of Otto cycle. For this purpose, we adopt the collision model and treat the reservoir as an ensemble of identically prepared two-level ancillas, which are also labeled as R_i for simplicity. The free Hamiltonian of generic ancilla R_i reads

$$\hat{H}_{R_i} = \frac{1}{2}\omega_i \hat{\sigma}_{R_i}^z \tag{1}$$

with ω_i the frequency of ancilla R_i and $\hat{\sigma}^{x,y,z}$ the usual Pauli operators. The nonthermal state of R_i can be described as a combination of both thermal and coherence terms that take on the form

$$\rho_{R_i} = \rho_{R_i}^{th} + \lambda_i \rho_{R_i}^{coh}, \tag{2}$$

in which $\rho_{R_i}^{th} = e^{-\beta_i \hat{H}_{R_i}}/Z_{R_i}$ is the canonical equilibrium thermal state at inverse temperature β_i with $Z_{R_i} = \mathrm{Tr}[e^{-\beta_i \hat{H}_{R_i}}]$ the partition function, $\rho_{R_i}^{coh}$ affords the coherent component of ρ_{R_i}, and the parameter $\lambda \in [0, 1]$ controls the magnitude of the coherence. We express thermal parts of the states of R_h and R_c as $\rho_{R_h}^{th} = p\,|1\rangle\langle 1| + (1-p)\,|0\rangle\langle 0|$ and $\rho_{R_c}^{th} = q\,|1\rangle\langle 1| + (1-q)\,|0\rangle\langle 0|$, respectively, with $p = [1 - \tanh(\beta_h\omega_h/2)]/2$, $q = [1 - \tanh(\beta_c\omega_c/2)]/2$, and $|1\rangle$ ($|0\rangle$) the excited (ground) state of the ancilla, while the coherent portion as $\rho_{R_i}^{coh} = (e^{i\phi_i}\,|1\rangle\langle 0| + e^{-i\phi_i}\,|0\rangle\langle 1|)/Z_{R_i}$.

We consider the quantum Otto cycle in a stationary regime where the system returns to its initial state after a complete cycle. The concrete processes, as schematically depicted in figure 1, can be described as follows:

Stroke I- adiabatic compression: in this process, the system is completely isolated from any reservoir, which means that no heat flows into or out of the system. The frequency of the system is gradually changed from ω_c to ω_h, and the corresponding Hamiltonian is also changed from $\hat{H}_S^c$ to $\hat{H}_S^h$. There is no restriction on the relationship between ω_c and ω_h and consequently, various operating regimes of the cycle can be achieved. It is assumed that the frequency change of the system is slow enough to keep the state of the system ρ_S^c unchanged during the process. The variations in the internal energy of the system can be attributed entirely to the work, which can be expressed as

$$W_1 = \mathrm{Tr}\left[\left(\hat{H}_S^h - \hat{H}_S^c\right)\rho_S^c\right]. \tag{3}$$

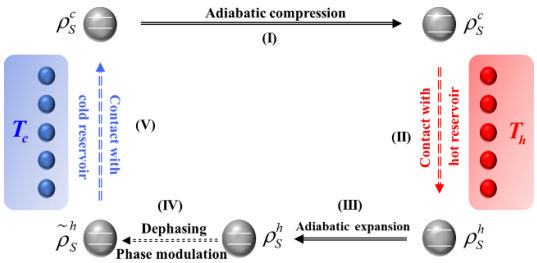

Figure 1. Schematic diagram of the Otto cycle. (I) and (III) are two adiabatic strokes in which the system is isolated from the reservoir and produce work through alteration of the system's frequency. (II) and (V) are two isochoric strokes with the system exchanging heat with the hot and cold reservoirs, respectively. An additional stoke (IV) is added to implement the dephasing and phase modulation operations on the system's steady state. In our model, the reservoirs are modeled as a series of identically prepared qubits that interact with the system sequentially. Our Otto cycle works in the stationary regime in the limit cycle.

Stroke II-contact with hot reservoir: during this stage, the system with a fixed Hamiltonian $\hat{H}_S^h$ is brought into contact with an ancilla R_h from the hot reservoir for a short time duration of τ_h. The system's state ρ_S^c is then transformed to $\rho_S^h = \mathrm{Tr}_{R_h}[\hat{U}_h \rho_S^c \otimes \rho_{R_h} \hat{U}_h^\dagger]$ with $\hat{U}_h = e^{-i\tau_h\left(\hat{H}_S^h + \hat{H}_{R_h} + \hat{V}_{SR_h}\right)}$ the unitary evolution operator and $\hat{V}_{SR_h}$ the interaction Hamiltonian. By constraining the energy conservation for the interaction in the sense of $[\hat{V}_{SR_h}, \hat{H}_S^h + \hat{H}_{R_h}] = 0$, the changes of internal energy of S originate completely from the heat exchanged with R_h given as

$$Q_H = \mathrm{Tr}\left[\hat{H}_S^h\left(\rho_S^h - \rho_S^c\right)\right]. \tag{4}$$

Notice that, the ancilla after interaction with the system is discarded and is replaced with a fresh one in the next round of cycle.

Stroke III-adiabatic expansion: in a similar manner to the first stroke, the system is completely isolated from any reservoir, and there is no heat exchange with the system. The frequency of the system is then changed from ω_h to ω_c, and the Hamiltonian changes from $\hat{H}_S^h$ to $\hat{H}_S^c$ accordingly. It is assumed that the system's state ρ_S^h remains preserved throughout the process. Therefore, any changes to the system's energy can be completely attributed to work, which is given as

$$W_2 = \mathrm{Tr}\left[\left(\hat{H}_S^c - \hat{H}_S^h\right)\rho_S^h\right]. \tag{5}$$

Stroke IV-dephasing and phase modulation operations: to reveal the impact mechanism of nonthermal reservoirs with coherence on the Otto cycle, we introduce dephasing and phase modulation operations on the system during the fourth stroke. We shall show that the magnitude and phase of the system's coherent state play a crucial role in various phenomena induced by the coherent reservoir. A dephasing operation is carried out in the energy basis of the system to eliminate the system's coherence. The strength of this operation is determined by a parameter $\alpha \in [0,1]$, with $\alpha = 0$ representing complete elimination of coherence and no operation being performed when $\alpha = 1$. Additionally, we perform phase modulation operations on the system to alter the functions of the cycle as thermal machines. Neither the dephasing operation nor the phase modulation affects the internal energy of the system, and thus, they do not have any energetic cost.

Stroke V-contact with cold reservoir: the system with fixed Hamiltonian $\hat{H}_S^c$ is put into contact with an ancilla R_c of the cold reservoir for a duration τ_c. The state of the system is transformed from ρ_S^h to $\rho_S^c = \mathrm{Tr}_{R_c}\left[\hat{U}_c \rho_S^h \otimes \rho_{R_c} \hat{U}_c^\dagger\right]$ with $\hat{U}_c = e^{-i\tau_c\left(\hat{H}_S^c + \hat{H}_{R_c} + \hat{V}_{SR_c}\right)}$ the time evolution operator and $\hat{V}_{SR_c}$ denoting the interaction between S and R_c. Assuming that the interaction $\hat{V}_{SR_c}$ conserves energy, the internal energy change of the system is equal to the heat exchanged with R_c, which is given as

$$Q_C = \mathrm{Tr}\left[\hat{H}_S^c\left(\rho_S^c - \rho_S^h\right)\right]. \tag{6}$$

We adopt the sign convention that the heat or work is positive when energy flows into the system. The Otto cycle has different operating regimes depending on the signs of the thermodynamic quantities. The cycle operating as an engine can be characterized by $Q_H > 0$, $Q_C < 0$ and $W_T = W_1 + W_2 < 0$ with the Otto efficiency

$$\eta = \frac{|W_T|}{Q_H} = 1 - \frac{\omega_c}{\omega_h}, \tag{7}$$

which is upper bounded by the Carnot efficiency $\eta_c = 1 - T_c/T_h$ for the usual engine. A refrigerator is achieved when $Q_H < 0$, $Q_C > 0$ and $W_T = W_1 + W_2 > 0$ whose coefficient of performance (COP) reads

$$COP = \frac{Q_C}{|W_T|} = \frac{\omega_c}{\omega_h - \omega_c}, \tag{8}$$

which is also upper bounded by the Carnot COP $COP_c = \frac{T_c}{T_h - T_c}$ for the usual refrigerator. The cycle can also act as an accelerator, in which the work is injected into the system and transformed into heat flowing to the cold reservoir along with the spontaneous heat from the hot reservoir. In addition to these three types of normal functions, namely, the engine with Otto efficiency, the refrigerator with Otto COP and the accelerator, we shall show that due to the existence of coherence in nonthermal reservoir, the cycle can achieve some anomalous functions that are impossible if only thermal reservoirs are involved. Moreover, by means of the dephasing and phase modulation operations in the fourth stroke, we point out that the steady-state coherence of the system plays a significant role in modifying the effect of nonthermal reservoir.

3. A qubit acts as working substance

We consider a situation where the working substance S is a qubit with the Hamiltonians alternating between $\hat{H}_S^h = \omega_h \sigma_S^+ \sigma_S^-$ and $\hat{H}_S^c = \omega_c \sigma_S^+ \sigma_S^-$ when interacts with the hot and cold reservoirs, respectively. The interacting Hamiltonian between S and reservoir R_i with $i = h, c$ is set as

$$\hat{V}_{SR_i} = J_i \left[\hat{\sigma}_S^x \hat{\sigma}_{R_i}^x + \hat{\sigma}_S^y \hat{\sigma}_{R_i}^y \right]. \tag{9}$$

We express the steady state of the system as $\rho_{ss}^c = \sum_{n,n'=0}^{1} \rho_{nn'} |n\rangle \langle n'|$ with $\rho_{nn'} = \langle n| \rho_{ss}^c |n'\rangle$, which fulfills the relation $\rho_{ss}^c = \mathrm{Tr}_{R_c}[\hat{U}_c \rho_{ss}^h \otimes \rho_{R_c} \hat{U}_c^\dagger]$ with $\rho_{ss}^h = \mathrm{Tr}_{R_h}[\hat{U}_h \rho_{ss}^c \otimes \rho_{R_h} \hat{U}_h^\dagger]$ the state after coupling with the hot reservoir. Therefore, in the whole cycle, the system bounces between the states ρ_{ss}^c and ρ_{ss}^h, as we have assumed that in the compression and expansion strokes the system's state remain unchanged. In the following, we consider two scenarios where one reservoir is in a coherent state while the other is in a thermal state. It turns out that different operating regimes can be achieved in each of these scenarios.

3.1. The cold reservoir is nonthermal

We first consider the situation where only the cold reservoir, R_c, is in the nonthermal state, as described by equation (2), and has a finite amount of coherence characterized by λ_c. The hot reservoir, R_h, on the other hand, is in the thermal state with an inverse temperature β_h, i.e. the state equation (2) with $\lambda_h = 0$.

3.1.1. The impact of coherence on operating regimes

In figure 2, we demonstrate the impact of coherence of R_c on the operating regimes of the Otto cycle temporarily without considering the dephasing operation and phase modulation in the fourth stroke. The plot showcases the variations of heat exchanged with the hot and cold reservoirs (Q_H and Q_C respectively) along with the total work W_T as a function of ω_h/ω_c. In figure 2(a), we can see a scenario where both the hot and cold reservoirs are in thermal states, denoted by $\lambda_c = \lambda_h = 0$. This serves as a benchmark for analyzing the effects of nonthermal reservoirs on the Otto cycle. We can see that there appear three operating regimes, which are determined by the values of ω_h/ω_c for given temperatures of two reservoirs. In the region where $0 < \omega_h/\omega_c < 1$, the cycle functions as an accelerator (labeled as A in the figure). In this phase, work is input to the system with $W_T > 0$ and at the same time, heat is transferred from R_h to R_c with $Q_H > 0$ and $Q_C < 0$. As the system enters the interval of $1 < \omega_h/\omega_c < T_h/T_c = 2$, it becomes an engine (labeled as E in the figure). During this phase, the system dumps a portion of the heat absorbed from R_h to R_c with $Q_H > 0$ and $Q_C < 0$ and supplies work to an external agent with $W_T < 0$. When thermal reservoirs are present, $\omega_h/\omega_c = T_h/T_c$ determines the Carnot point, at which the cycle operates as a machine with maximum efficiency, known as the Carnot efficiency, and both the heat and work are zero. As the cycle passes the Carnot point, i.e. $\omega_h/\omega_c = T_h/T_c = 2$ in the present case, it transforms into a refrigerator (labeled as R in the figure) in which work is consumed to transfer heat from R_c to R_h with $Q_H < 0$, $Q_C > 0$, and $W_T > 0$.

Figure 2(b) deals with the nonthermal R_c with $\lambda_c = 0.2$, from which we can see that when $1.18 < \omega_h/\omega_c < T_h/T_c = 2$, an abnormal refrigerator appears with a COP larger than the Carnot COP COP_c. This is called a super-refrigerator and labeled as sup-R in the figure. By increasing the coherence of R_c to $\lambda_c = 0.4$, as shown in figure 2(c), we acquire a hybrid refrigerator which can perform work for an external agent while simultaneously transferring heat from R_c to R_h (labeled as HR in the figure). In figure 2(c), the super-refrigerator also appears within $1 < \omega_h/\omega_c < T_h/T_c = 2$, which is the entire region where the usual engine appears in the presence of thermal reservoirs as depicted in figure 2(a). For both $\lambda_c = 0.2$ and $\lambda_c = 0.4$, the normal refrigerator is recovered for $\omega_h/\omega_c > T_h/T_c = 2$.

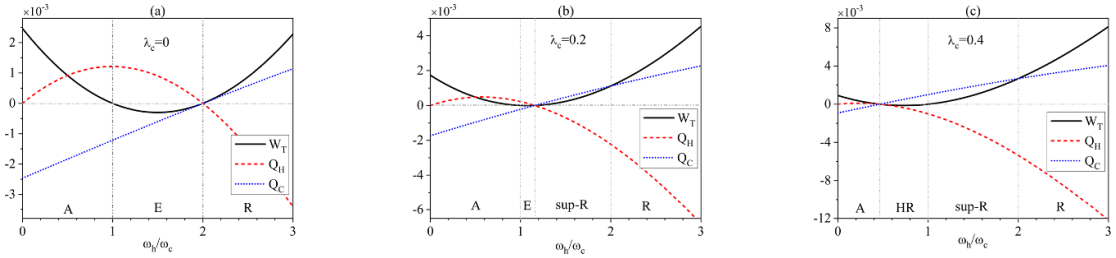

Figure 2. The heat Q_H and Q_C, and total work W_T as a function of ω_h/ω_c for the situation where only the cold reservoir is nonthermal with $\lambda_c = 0$ (a), $\lambda_c = 0.2$ (b), and $\lambda_c = 0.4$ (c). The functions as an accelerator, an engine, a refrigerator, a super-refrigerator and a hybrid refrigerator are marked as A, E, R, sup-R and HR in the figure. The other parameters are set as $\lambda_h = 0$, $T_h = 4\omega_c$, $T_c = 2\omega_c$, $J_h = J_c = 10\omega_c$ and $\tau_h = \tau_c = 0.01$.

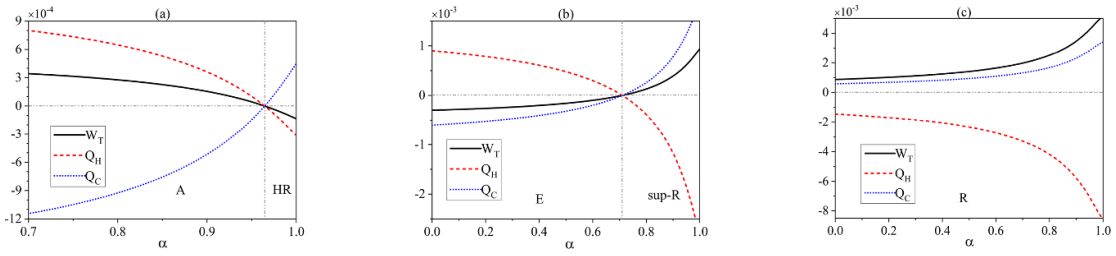

Figure 3. The heat Q_H and Q_C, and total work W_T as a function of dephasing strength in terms of α for $\omega_h/\omega_c = 0.7$ (a), $\omega_h/\omega_c = 1.5$ (b), and $\omega_h/\omega_c = 2.5$. The functions as an accelerator, an engine, a refrigerator, a super-refrigerator and a hybrid refrigerator are marked as A, E, R, sup-R and HR in the figure. The other parameters are set as $\lambda_c = 0.4$, $\lambda_h = 0$, $T_h = 4\omega_c$, $T_c = 2\omega_c$, $J_h = J_c = 10\omega_c$ and $\tau_h = \tau_c = 0.01$.

3.1.2. The effect of dephasing operation

It has been observed that the anomalous functions of the Otto cycle are induced by coherences in the nonthermal reservoir. On the other hand, the magnitude and phase of coherence in the system also play a significant role in these phenomena. To further clarify this observation, we subject the system to dephasing and phase modulation operations during the fourth stroke. By denoting the strength of the dephasing with a parameter α and introducing the phase φ_s, the state of the system after the fourth stroke can be expressed as $\tilde{\rho}_{ss}^h = r_{11}|1\rangle\langle 1| + r_{00}|0\rangle\langle 0| + \alpha\left(r_{10}e^{i\varphi_s}|1\rangle\langle 0| + r_{01}e^{-i\varphi_s}|0\rangle\langle 1|\right)$ with $r_{nn'} = \langle n|\tilde{\rho}_{ss}^h|n'\rangle$. The equations governing the steady state of the system can be derived as

$$f_1\rho_{11} + f_2\rho_{00} + \lambda_c\alpha\left(f_3\rho_{10} + h.c.\right) = 0, \tag{10}$$

$$\lambda_c g_1\rho_{11} + \lambda_c g_2\rho_{00} + \left(\alpha g_3 - 1\right)\rho_{10} = 0, \tag{11}$$

$$\lambda_c g_1^*\rho_{11} + \lambda_c g_2^*\rho_{00} + \left(\alpha g_3^* - 1\right)\rho_{01} = 0, \tag{12}$$

with the coefficients f_1, f_2, f_3, g_1, g_2 and g_3 are given in appendix.

According to equation (10), if both λ_c and α are nonzero, then the coherence and populations of the system are coupled to each other, which means that coherence behaves as populations, and consequently, affects the energy of the system. It also indicates that the coherence of the nonthermal reservoir and that of the system work together in the sense that the existence of system's steady-state coherence is necessary for the coherence of the nonthermal reservoir to effectively contribute to the system's energy variation and ultimately, the cycle's operating regimes. This can be seen by setting $\alpha = 0$, i.e. a complete dephasing for the system, which makes the dynamics of the system's populations and thus energy exchanges immune to the coherence of the reservoir. As a consequence, the coherence of the nonthermal reservoir no longer has any influence on the system's thermodynamics.

For a more intuitive display, we plot the dependence of Q_H, Q_C, and W_T on the dephasing strength α in figure 3. Keep in mind that $\alpha = 1$ represents no dephasing, while $\alpha = 0$ represents complete dephasing on the system. We consider the situation of $\lambda_c = 0.4$ as exhibited in figure 2(c) and select different values of ω_h/ω_c therein. Figure 3(a) is for $\omega_h/\omega_c = 0.7$ corresponding to the emergence of the hybrid refrigerator if no dephasing operation exists with $\alpha = 1$. It is important to note that the hybrid refrigerator can still function within the relatively weak dephasing operations range of $0.96 < \alpha < 1$. However, the relatively strong dephasing operations with $0 \leqslant \alpha < 0.96$ turn the hybrid refrigerator into an accelerator emerging in the thermal reservoir with $\lambda_c = 0$, as shown in figure 2(a). In figure 3(b), we select $\omega_h/\omega_c = 1.5$, which

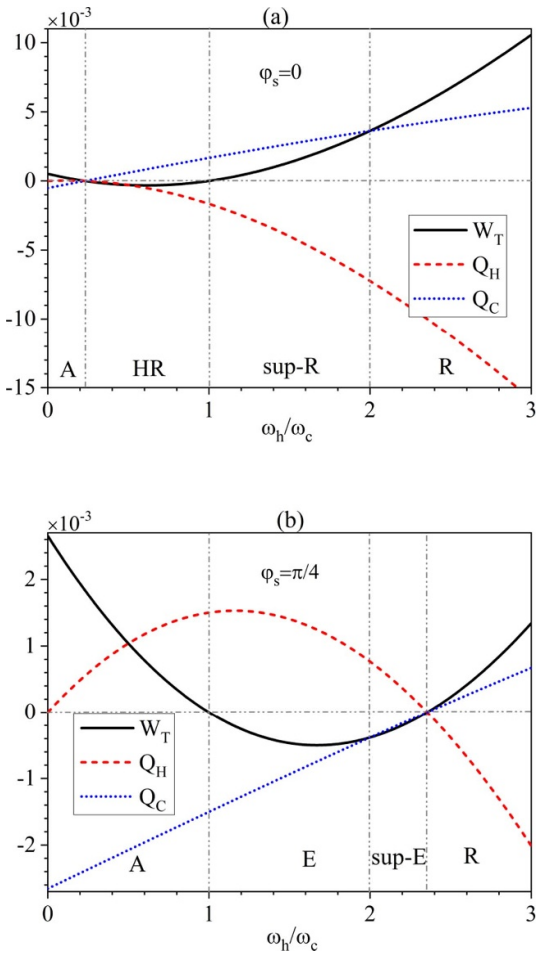

Figure 4. The heat Q_H and Q_C, and total work W_T as a function of ω_h/ω_c for different phases of system's steady-state set at the fourth stroke with $\varphi_s = 0$ (a) and $\varphi_s = \pi/4$ (b). The functions as an accelerator, an engine, a refrigerator, a super-refrigerator, a hybrid refrigerator and a sup-engine are marked as A, E, R, sup-R, HR and sup-E in the figure. The other parameters are set as $\lambda_c = 0.6$, $\alpha = 1$, $\lambda_h = \phi_h = 0$, $\phi_c = 0$, $T_h = 4\omega_c$, $T_c = 2\omega_c$, $J_h = J_c = 10\omega_c$ and $\tau_h = \tau_c = 0.01$.

corresponds to the super-refrigerator in figure 2(c), in the absence of the dephasing operation with $\alpha = 1$. It is important to note that even with dephasing operation where $0.71 < \alpha < 1$, the super-refrigerator can still woke. However, if we increase the dephasing strength to the interval of $0 \leqslant \alpha < 0.71$, the super-refrigerator will transform into the usual engine that appears in the thermal reservoir, as illustrated in figure 2(a). Therefore, the unusual operations of the cycle that are caused by the coherence of the nonthermal reservoir can be prevented by applying a relatively strong dephasing operation on the system. This causes the cycle to transition to the normal operation states that occur in the thermal reservoirs.

From figures 3(a) and (b), we also notice that in those normal regimes recovered by the dephasing operation, i.e. $0 \leqslant \alpha < 0.96$ in figure 3(a) and $0 \leqslant \alpha < 0.71$ in figure 3(b), the performances of the cycle is enhanced by increasing the dephasing strength (i.e. decreasing the values of α), or, alternatively, reducing the coherence of steady-state of the system. Specifically, both the dumped heat Q_C to the cold reservoir in the accelerator, figure 3(a), and the supplied work W_T in the engine, figure 3(b), are proportional to the dephasing strength. It may seem like coherence has a negative impact on the cycle's performance, but the truth is that its effect depends on specific circumstances. In fact, if we operate the cycle as a normal refrigerator with $\omega_h/\omega_c = 2.5$, as shown in figure 2(c), the dephasing of coherence can actually degrade the cycle's performance, as illustrated in figure 3(c). It is observed that an increase in dephasing strength leads to a decrease in cooling power Q_C. Therefore, coherence can either hinder or facilitate the performance of the Otto cycle, depending on the chosen parameters.

3.1.3. The effect of phase modulation

In our Otto cycle model, we have added an extra stroke to modify the phase φ_s of the system's steady-state, apart from performing the dephasing operation. Our objective is to study how the phase φ_s impacts the functions of the Otto cycle. We plot Q_H, Q_C, and W_T as a function of ω_h/ω_c for $\varphi_s = 0$ and $\varphi_s = \pi/4$ for $\lambda_c = 0.6$ in figure 4. From figure 4(a), we observe four operating regimes of the cycle, namely, the accelerator,

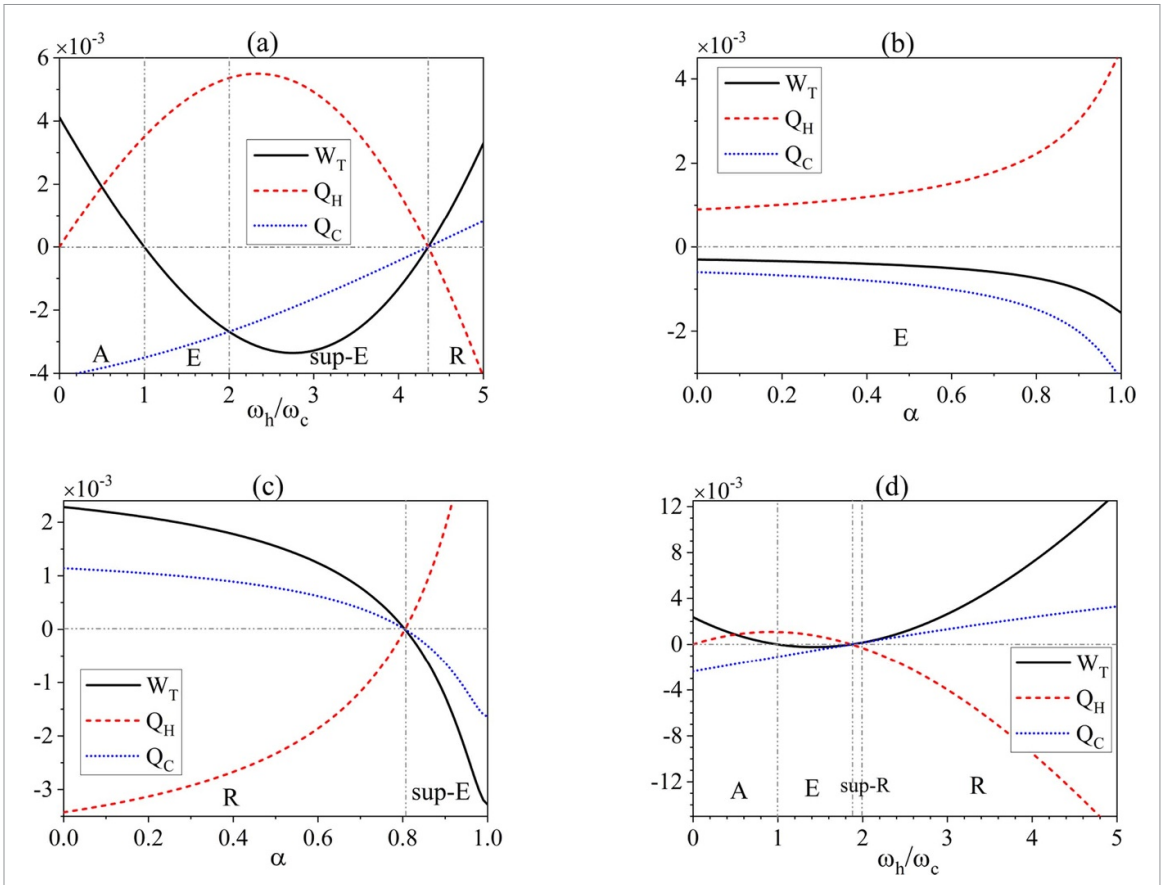

Figure 5. The hot reservoir is in nonthermal state with a finite nonzero coherences. (a) The heat Q_H and Q_C, and total work W_T as a function of ω_h/ω_c without the dephasing operation with $\alpha = 1$ and for $\varphi_s = 0$. The dependence of Q_H, Q_C and W_T on dephasing strength α for $\omega_h = 1.5\omega_c$ (b) and $\omega_h = 3\omega_c$ (c) for $\varphi_s = 0$. (d) Q_H, Q_C and W_T versus ω_h/ω_c for $\alpha = 1$ and $\varphi_s = \pi/4$. The functions as an accelerator, an engine, a refrigerator, a super-refrigerator and a super-engine are marked as A, E, R, sup-R and sup-E in the figure. The other parameters are given as $\lambda_c = \phi_c = 0$, $\lambda_h = 0.4$, $T_h = 4$, $T_c = 2$, $J_h = J_c = 10\omega_c$ and $\tau_h = \tau_c = 0.01$.

hybrid refrigerator, super-refrigerator, and refrigerator, for $\varphi_s = 0$, which is similar to the display in figure 2(c) with $\lambda_c = 0.4$. For $\varphi_s = \pi/4$, as depicted in figure 4(b), the hybrid refrigerator and super-refrigerator no longer exist, and the engine and super-engine arise. The intervals for the accelerator and refrigerator are also altered. This clearly demonstrates the effects of the phase of the system's steady-state on the cycle's operating regimes, thus providing a method to achieve the desired functions.

3.2. The hot reservoir is nonthermal

We then proceed to the configuration where only the hot reservoir R_h is prepared in the nonthermal state given in equation (2), while the cold reservoir R_c is in the thermal state with inverse temperature β_c. We illustrate the operating regimes of the Otto cycle by plotting in figure 5(a) the heat Q_H and Q_C, and the total work W_T with respect to ω_h/ω_c for $\lambda_h = 0.4$ regarding coherence in R_h. For the time being, we take no account of the dephasing operation with $\alpha = 1$ and set $\varphi_s = 0$ in the fourth stroke. The cycle's behavior is determined by the ratio of ω_h/ω_c, and can be classified into four regions: $0 < \omega_h/\omega_c < 1$, $1 < \omega_h/\omega_c < 2$, $2 < \omega_h/\omega_c < 4.35$ and $\omega_h/\omega_c > 4.35$. In the first and second regions, the cycle functions as an accelerator and an engine, respectively, which is similar to the behavior of the cycle when both reservoirs are in thermal states, as shown in figure 2(a). When the cycle crosses the Carnot point, $\omega_h/\omega_c = T_h/T_c = 2$, it still functions as an engine. However, its efficiency exceeds the Carnot limit, $\eta > \eta_c$, due to the existence of coherence in reservoir R_h. This engine is called a super-engine, denoted by sup-E in the figure, to distinguish it from the usual engine. Finally, by further increasing ω_h/ω_c, the cycle returns to functioning as a normal refrigerator.

We now include the dephasing operation and phase modulation in the fourth stroke and express the system's state after which as $\tilde{\rho}_{ss}^h = r_{11}|1\rangle\langle 1| + r_{00}|0\rangle\langle 0| + \alpha\left(r_{10}e^{i\varphi_s}|1\rangle\langle 0| + r_{01}e^{-i\varphi_s}|0\rangle\langle 1|\right)$. The equations governing the system's steady state reads

$$f_1\rho_{11} + f_2\rho_{00} + \lambda_h\left(f_3'\rho_{10} + h.c.\right) = 0, \tag{13}$$

$$\lambda_h\alpha g_1'\left(\rho_{11} - \rho_{00}\right) + \left(\alpha g_2' - 1\right)\rho_{10} = 0, \tag{14}$$

$$\lambda_h\alpha g_1'^*\left(\rho_{11} - \rho_{00}\right) + \left(\alpha g_2'^* - 1\right)\rho_{01} = 0, \tag{15}$$

in which the expressions of f_1 and f_2 are the same as that given in equation (10), while f_3', g_1' and g_2' are given in appendix.

The above equations indicate that only when $\lambda_h \neq 0$ and $\alpha \neq 0$ are satisfied at the same time can the coherence of the system make contribution to the populations and eventually to the energy variations. In other words, if the dephasing operation in the fourth stroke completely erases the coherence of the system with $\alpha = 0$, the coherence of nonthermal hot reservoir, even if exists, does not work at all. In the following, we shall demonstrate the effects of coherences of system's steady state on the performances of the Otto cycle by varying the dephasing strength α. We also exhibit how the phase modulation of system's steady state affects the functions of the cycle.

In figures 5(b) and (c), we show the dependence of thermodynamic quantities on the strength of dephasing operation in terms of α for $\lambda_h = 0.4$. This enables us to compare the results with those obtained in figure 5(a) without the dephasing with $\alpha = 1$. In figure 5(b), we first consider $\omega_h/\omega_c = 1.5$ for which the cycle operates as a usual engine if no dephasing is involved (cf figure 5(a)). The function of an engine is retained after introducing the dephasing operation but the work done to the external agent is shrunk by increasing the dephasing strength, i.e. changing α from 1 to 0, as manifested figure 5(b). We then consider $\omega_h/\omega_c = 3$ in figure 5(c), leading the cycle to the regime of super-engine without the dephasing (cf figure 5(a)). The relatively weak dephasing with $0.81 \leqslant \alpha \leqslant 1$ can still keep the super-engine functionality of the cycle, as shown in figure 5(c). However, for the relatively strong dephasing with $0 \leqslant \alpha < 0.81$, the super-engine is transformed into the refrigerator. We also observe that the power of the refrigerator in terms of Q_C is increased by strengthening the dephasing operation, i.e. changing α from 0.81 to zero. Therefore, the dephasing operation can not only improve but also suppress the performances of the cycle relying on the regions of parameters we consider.

Apart from the dephasing operation, we can also alter the cycle's functions by modulating the system's phase during the fourth stroke. For instance, if we set φ_s to $\pi/4$ and remove the dephasing operation with $\alpha = 1$, as shown in figure 5(d), the super-engine that was initially present for $\varphi_s = 0$ (cf figure 5(a)) disappears and a new function of super-refrigerator emerges.

3.3. The decomposition of thermodynamic quantities

In the aforementioned discussions, we have detailed the operating regimes of the Otto cycle when there is a coherent nonthermal reservoir present. Moreover, we have demonstrated how the performances of the Otto cycle as thermal machines are altered by the dephasing operation and phase modulation on the system during the additional fourth stroke. In the following, we further investigate the concrete ways in which coherence of nonthermal reservoir affects the Otto cycle to shed some light on the emergence of anomalous functions. We observe that the influences of reservoir's coherence include two aspects: one is the steady-state coherence and population of the system, and the other is the direct impact on energy exchange when the system interacts with the nonthermal reservoir. The impact on system's steady-state populations alters its temperature, which in turn changes the exchanged energy with two reservoirs and eventually the functions of the cycle. In addition to that, the coherence of nonthermal reservoir, along with the steady-state coherence of the system, can be coupled to the system's populations in the interaction between the system and reservoir, which implies the coherences behave as populations and directly contributing to the energy exchange and operating regimes of the cycle. This aspect has also been embodied in the previous discussions that, by modifying the system's coherence, the operating regimes of the cycle will be changed.

To formulate this observation, we decompose the thermodynamic quantities into contributions from populations and coherence of the system focusing on an instance where only the hot reservoir is nonthermal. The exchanged heat Q_H with the hot reservoir can be split into Q_H^{pop} and Q_H^{coh}, i.e. the contributions from populations and coherence of the system, and derived as

$$Q_H^{pop} = \omega_h \sin^2(2J_h\tau_h)(p - \rho_{11}) \tag{16}$$

and

$$Q_H^{coh} = \frac{1}{4}\omega_h\lambda_h \mathrm{sech}(\omega_h/2T_h)\sin[4J_h\tau_h] \times [-2\mathrm{Im}(\rho_{10})\cos\phi_h + 2\mathrm{Re}(\rho_{10})\sin\phi_h]. \tag{17}$$

In equation (16), although only the parameter p characterizing the thermal part of the nonthermal state of R_h appears, the effects of coherence of R_h has entered the populations ρ_{11} of the system. From equation (17), we notice only when both the coherence of the nonthermal reservoir and that of the system exist, i.e. $\lambda_h \neq 0$ and meanwhile $\rho_{10} \neq 0$, can the associated coherences make a direct contribution to the heat. Since the cold reservoir R_c is assumed to be thermal with $\lambda_c = 0$, the system's coherence will not affect the heat Q_C, or, alternatively, Q_C is completely contributed by the system's populations. However, in this case, the coherence

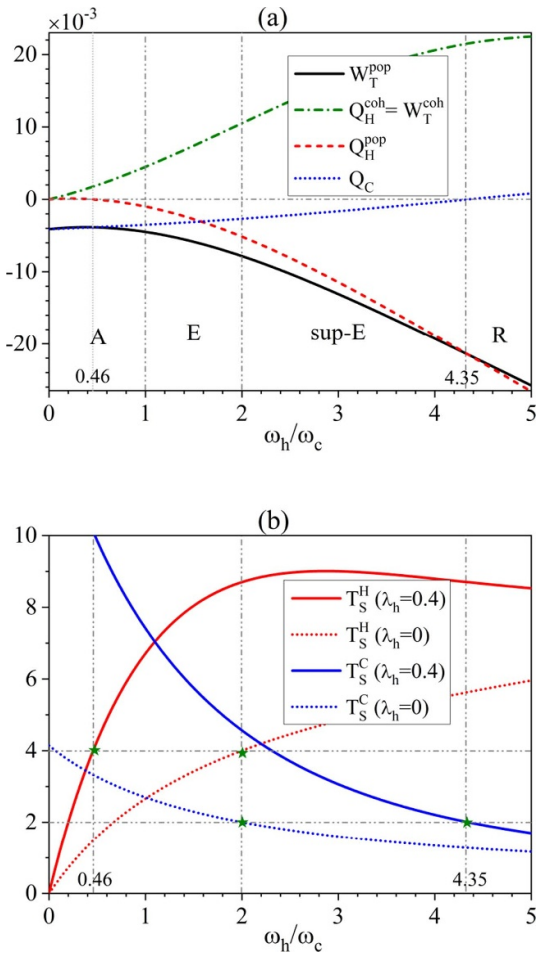

Figure 6. (a) The decomposed heat Q_H^{pop} and Q_H^{coh}, and work W_T^{pop} and W_T^{coh} contributed by system's populations and coherence, respectively, as well as Q_C as a function of ω_h/ω_c for $\lambda_h = 0.4$. (b) The system's temperatures T_S^H and T_S^C before interacting with the hot and cold reservoirs, respectively, versus ω_h/ω_c for $\lambda_h = 0$ and $\lambda_h = 0.4$. The functions as an accelerator, an engine, a refrigerator and a super-engine are marked as A, E, R and sup-E in the figure. The other parameters are set as $\lambda_c = \phi_c = 0$, $\phi_h = 0$, $T_h = 4\omega_c$, $T_c = 2\omega_c$, $\alpha = 1$, $\varphi_s = 0$, $\phi_h = 0$, $J_h = J_c = 10\omega_c$ and $\tau_h = \tau_c = 0.01$.

of the hot reservoir can still influence the heat Q_C via the system's populations. As the work is given by the unbalance of the heat Q_H and Q_C, it can be decomposed into two components $W_T^{pop} = Q_H^{pop} + Q_C$ and $W_T^{coh} = Q_H^{coh}$ that is due to the populations and coherence of the system's steady-state, respectively.

In figure 6(a), we exhibit the decomposed thermodynamics quantities Q_H^{pop}, Q_H^{coh}, W_T^{pop} and W_T^{coh} as well as heat Q_C for $\lambda_h = 0.4$ and the same other parameters used in figure 5(a). That is, figure 6(a) displays the decomposed components for Q_H and W_T in figure 5(a), while Q_C is identical in both figures.

In order to show the impacts of reservoir's coherence on the system's steady-state populations, we concentrate on the system's temperatures defined as $T_S = \omega_S/\ln(\rho_g/\rho_e)$ with ω_S the energy gap and $\rho_g(\rho_e)$ the ground (excited) state populations. In figure 6(b), we plot the temperatures of the system before interacting with the hot and cold reservoirs, labeled as T_S^H and T_S^C, respectively, for $\lambda_h = 0.4$ and $\lambda_h = 0$. We can see that in comparison to $\lambda_h = 0$, the presence of coherence of R_h greatly modify T_S^H and T_S^C. In particular, $T_S^H > T_h = 4$ is achieved when $\omega_h/\omega_c > 2$ is met for $\lambda_h = 0$, which becomes $\omega_h/\omega_c > 0.46$ for $\lambda_h = 0.4$. Similarly, $T_S^C < T_c = 2$ is achieved when $\omega_h/\omega_c > 2$ is met for $\lambda_h = 0$, which is then extended to $\omega_h/\omega_c > 4.35$ for $\lambda_h = 0.4$. We have marked the critical points by stars in the figure. This effect of coherence on steady-state populations is reflected in figure 6(a), from which we can see that the component Q_H^{pop} becomes negative at the point $\omega_h/\omega_c = 0.46$ at which $T_S^H > T_h$, and at the same time Q_C becomes positive at the point $\omega_h/\omega_c = 4.35$ at which $T_S^C < T_c$.

The anomalous function of the cycle is the super-engine appearing in the region $2 < \omega_h/\omega_c < 4.35$ with $W_T < 0$, $Q_H > 0$ and $Q_C < 0$, as shown in figure 5(a), whose specific contributions can now be observed in figure 6(a). It is clear that W_T is determined by W_T^{pop} as they have the same signs, while W_T^{coh} has the opposite sign to W_T and thus suppresses W_T. By contrast, Q_H^{coh} determines the positive Q_H, while Q_H^{pop} reduces it.

4. Two qubits act as working substance

In this section, we discuss the configuration where the working substance S is composed of two identical qubits, namely S_1 and S_2. In this scenario, the reservoir is common to the two qubits, which allows for the generation of degenerate coherence during their interaction with the reservoir. It allows us to compare the impact of a single qubit's energetic coherence versus the degenerate coherence of two qubits on the performance of the Otto cycle. The Hamiltonian of the system alternates between $\hat{H}_S^h = \omega_h(\sigma_{S_1}^+\sigma_{S_1}^- + \sigma_{S_2}^+\sigma_{S_2}^-)$ and $\hat{H}_S^c = \omega_c(\sigma_{S_1}^+\sigma_{S_1}^- + \sigma_{S_2}^+\sigma_{S_2}^-)$ when interacts with the hot and cold reservoirs R_h and R_c, respectively. This also means that the frequencies of the two qubits change identically during the work strokes. The interacting Hamiltonian between S and reservoir R_i with $i = h, c$ is taken to be

$$\hat{V}_{SR_i} = J_i\left[\left(\hat{\sigma}_{S_1}^x + \hat{\sigma}_{S_2}^x\right)\hat{\sigma}_{R_i}^x + \left(\hat{\sigma}_{S_1}^y + \hat{\sigma}_{S_2}^y\right)\hat{\sigma}_{R_i}^y\right]. \tag{18}$$

The steady state of the system can be expressed as $\rho_{ss}^c = \sum_{m,n,m',n'=0}^{1}\rho_{mn,m'n'}\left|mn\right\rangle\left\langle m'n'\right|$ with $\rho_{mn,m'n'} = \left\langle mn\right|\rho_{ss}^c\left|m'n'\right\rangle$, which fulfills the relation $\rho_{ss}^c = \mathrm{Tr}_{R_c}[\hat{U}_c\rho_{ss}^h \otimes \rho_{R_c}\hat{U}_c^\dagger]$ with $\rho_{ss}^h = \mathrm{Tr}_{R_h}[\hat{U}_h\rho_{ss}^c \otimes \rho_{R_h}\hat{U}_h^\dagger]$ the state after coupling with the hot reservoir. In a similar manner to a single qubit, the system oscillates between two states, ρ_{ss}^c and ρ_{ss}^h, throughout the cycle due to the assumption that the system's state remains unchanged during the compression and expansion strokes.

In the presence of nonthermal reservoir with energetic coherence, the steady state of the two qubits will contain both energetic and degenerate coherences. Therefore, we introduce the parameters α and γ to denote the strengths of the dephasing on the energetic and degenerate coherences, respectively. The state of the system after the dephasing operation can be expressed as

$$\begin{aligned}\tilde{\rho}_{ss}^h = &\sum_{m,n=0}^{1} r_{mn,mn}\left|mn\right\rangle\left\langle mn\right| + \alpha\left(\sum_{\substack{m,n,n'=0\\(n\neq n')}}^{1} r_{mn,mn'}\left|mn\right\rangle\left\langle mn'\right|\right.\\ &+\sum_{\substack{m,n,m'=0\\(m\neq m')}}^{1} r_{mn,m'n}\left|mn\right\rangle\left\langle m'n\right| + \left.\sum_{\substack{m,n,m',n'=0\\(m=n\neq m'=n')}}^{1} r_{mn,m'n'}\left|mn\right\rangle\left\langle m'n'\right|\right)\\ &+\gamma\sum_{\substack{m,n,m',n'=0\\(m\neq n,m'\neq m,n'\neq n)}}^{1} r_{mn,m'n'}\left|mn\right\rangle\left\langle m'n'\right|\end{aligned} \tag{19}$$

with $r_{ab,cd} = \left\langle ab\right|\tilde{\rho}_{ss}^h\left|cd\right\rangle$.

In the following, we will explore two scenarios: first, when both reservoirs are thermal, to demonstrate that the degenerate coherence of two qubits can affect the cycle even in the presence of thermal reservoirs. This is in stark contrast to the energetic coherence of a single qubit. Second, we will examine the impact of the coherence of non-thermal reservoir on the cycle. We note that the reservoir's coherence affects the cycle through the energetic steady-state coherence of the system, but is not related to the degenerate coherence.

We first focus on the effect of degenerate coherence of two qubits acting as working substance on the performance of Otto cycle when both reservoirs are prepared in thermal states. In this case, there appear three normal functions for the cycle, namely, the accelerator, the engine and the refrigerator, as shown in figure 7(a). It's worth noting that these operating regimes are identical to those obtained for a single qubit being exposed to two thermal reservoirs, as seen in figure 2(a). However, there is a difference between the steady state of a single qubit and that of two qubits, namely, the single qubit is in a thermal state, while two qubits have degenerate coherence due to simultaneous interactions with the common reservoirs. This degenerate coherence has a significant impact on the performance of the Otto cycle. Figures 7(b)–(d) demonstrate this effect for the cases of complete dephasing ($\gamma = 0$) and no dephasing ($\gamma = 1$) operations on the degenerate coherence. We use the dumped heat Q_C to the cold reservoir, the work W_T performed on an external agent, and the absorbed heat Q_C from the cold reservoir to characterize the cycle's performance as an accelerator, an engine, and a refrigerator, respectively. We observe that the presence of degenerate coherence, denoted by dashed lines in figures 7(b)–(d), always enhances these figures of merit when compared with complete dephasing, denoted by solid lines in the figures.

In figure 8, we have depicted the different operating regimes of the cycle when only the cold reservoir is in a nonthermal state. Interestingly, we found that the operating regimes of this scenario, namely, the

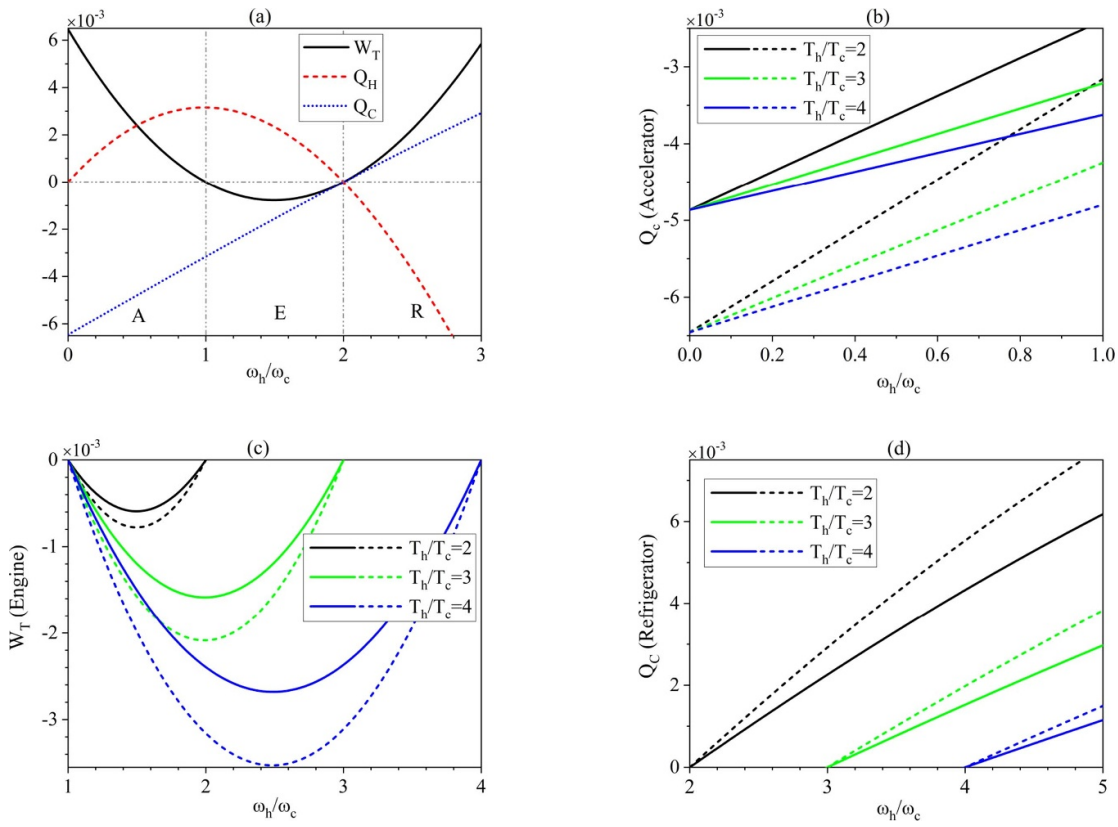

Figure 7. The scenario where both the two reservoirs are in thermal states and the working substance is two qubits. (a) The thermodynamic quantities Q_H, Q_C and W_T as a function of ω_h/ω_c for $T_h = 4$ and $T_c = 2$ without the dephasing and phase modulation operations. The functions as the accelerator, the engine and the refrigerator are marked as A, E and R in the figure. (b)–(d) display Q_C for the accelerator, W_T for the engine, and Q_C for the refrigerator versus ω_h/ω_c for the absence of dephasing with $\gamma = 1$ (dashed lines) and complete dephasing with $\gamma = 0$ (solid lines) for different temperatures of the two reservoirs. The other parameters are set as $J_h = J_c = 10\omega_c$ and $\tau_h = \tau_c = 0.01$.

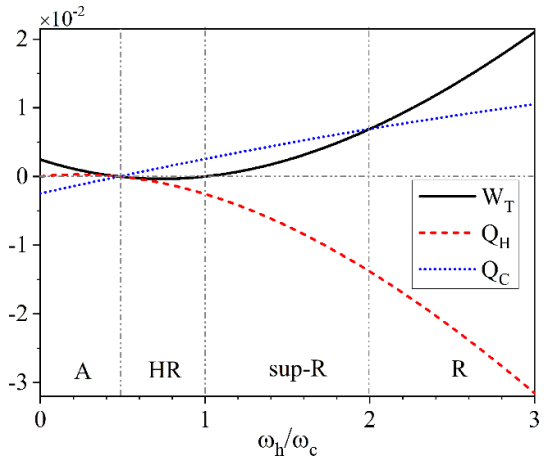

Figure 8. The scenario of two qubits as working substance. The thermodynamic quantities Q_H, Q_C and W_T as a function of ω_h/ω_c for the cold reservoir being nonthermal with $\lambda_c = 0.4$. The functions as the accelerator, hybrid refrigerator, super-refrigerator and refrigerator are marked as A, HR, sup-R and R in the figure. The other parameters are set as $T_h = 4$, $T_c = 2$, $J_h = J_c = 10\omega_c$, $\tau_h = \tau_c = 0.01$, $\lambda_h = 0$ and $\alpha = \gamma = 1$.

accelerator, the hybrid refrigerator, the super-refrigerator and the refrigerator, are the same as those for the case where a single qubit serves as the working substance, as shown in figure 2(c). This observation suggests that the underlying mechanism behind the emergence of these operating regimes, in particular the abnormal functions of hybrid refrigerator and super-refrigerator, is still due to the joint effects of the energetic coherence of the nonthermal state of the reservoir and the steady-state of the system, rather than the system's degenerate coherence. To verify this observation, we completely erase the energetic coherence of the system

with $\alpha = 0$, and find that the operating regimes of the cycle are changed into identical situation as those shown in figure 7(a) namely, the situation where two qubits are working in two thermal reservoirs. Therefore, the coherence in nonthermal reservoir exerts impact on the cycle through energetic coherence of the system in the steady state, which is irrelated to the system's degenerate coherence.

5. Conclusion

In conclusion, we have studied the effects of energetic coherence in nonthermal reservoir on the performance of Otto cycle. We first focus on the situation where a single qubit acts as the working substance. It is found that in comparison to the situations with thermal reservoirs, various abnormal operating regimes arise due to the existence of reservoir's coherence. For example, the cycle can function as heat engine and refrigerator but with the efficiency and COP surpassing the Carnot limits, and as hybrid refrigerator that can transfer the heat from cold reservoir to the hot one and simultaneously perform work to the external agent. We examine the influential mechanism of the nonthermal reservoir on the cycle by adding an extra stroke where the dephasing operation and phase modulation are performed on the system. It turns out that the amount of energetic coherence of system's steady-state and its phase play an important role in determining the functions of the cycle. This provides an efficient method to modify the cycle to achieve desired functions on the one hand, and on the other hand it indicates that the existence of system's steady-state energetic coherence is necessary for the reservoir's energetic coherence to exert influence on the cycle. If the energetic coherence of system's steady-state is erased completely, the nonthermal reservoir no longer has any impacts on the cycle.

We also study specific contributions of the nonthermal reservoir by decomposing the thermodynamic quantities into the components originating from populations and coherence of the system. We notice that the coherence of nonthermal reservoir alter the operating regimes of the cycle from two aspects, one is the modification of populations and temperature of the system and the other is the direct contribution to the heat in the interaction between the system and reservoirs.

We then consider the configuration where the working substance are two qubits and the degenerate coherence can be produced by interactions with the common reservoir. We show that the degenerate coherence can promote the figures of merit of the machines even when both reservoirs are in thermal states. In this sense, using more qubits as the working substance may bring more advantages [77], which is worth a deep exploration in the future. The energetic coherence of the reservoir influences the cycle still through the energetic coherence of the system, and is not related to the degenerate coherence. Our findings not only demonstrate the abilities of the coherence of nonthermal reservoir in powering the Otto cycle for various functions, but also provide insights into the mechanisms by which energetic coherence can play an effective role.

When implementing the Otto cycle in a thermal environment, solid-state quantum systems like trapped ions [78–80], nuclear magnetic resonance (NMR) techniques [16], and nitrogen-vacancy centers [14] are generally chosen as working substances. In our scheme, the working substance should be coupled to nonthermal reservoirs that contain a finite, nonzero coherence. This could pose a significant challenge to the implementation of the scheme in an experiment. We suggest utilizing a single-mode cavity field as the working substance, while solid-state systems like ions are used to achieve the coherent reservoir [81]. According to the concept of the photon-Carnot engine proposed by Scully *et al* [41], the process involves the random injection of ions into the cavity field, where they interact with the field. This interaction results in the exchange of heat between the nonthermal reservoir and the system during the thermal stroke.

Data availability statement

All data that support the findings of this study are included within the article (and any supplementary files).

Acknowledgments

This work was supported by National Natural Science Foundation (China) under Grant Nos. 11974209 and 12274257, Natural Science Foundation of Shandong Province (China) under Grant No. ZR2023LLZ015, Taishan Scholar Project of Shandong Province (China) under Grant No. tsqn201812059.

Appendix. The coefficients of equations governing the steady-state of the system

The coefficients for equations (10)–(12) are given as

$$
\begin{aligned}
f_1 &= \frac{1}{4}\left[-3+p+2q+(1+p-2q)\cos\left(4J_c\tau_c\right)-2\left(-1+p\right)\cos^2\left(2J_c\tau_c\right)\cos\left(4J_h\tau_h\right)\right],\\
f_2 &= \frac{1}{4}\left[p+2q+(p-2q)\cos\left(4J_c\tau_c\right)-2p\cos^2\left(2J_c\tau_c\right)\cos\left(4J_h\tau_h\right)\right],\\
f_3 &= \frac{1}{2}\left[\cos\left(2J_h\tau_h\right)\sin\left(4J_c\tau_c\right)\left(i\cos\left(\phi_c+\varphi_s+\tau_h\omega_h\right)+\sin\left(\phi_c+\varphi_s+\tau_h\omega_h\right)\right)\right]/Z_{R_c},\\
g_1 &= ie^{i\left(\phi_c-\tau_c\omega_c\right)}\left[p+(1-p)\cos\left(4J_h\tau_h\right)\right]\sin\left(2J_c\tau_c\right)/Z_{R_c},\\
g_2 &= -ie^{i\left(\phi_c-\tau_c\omega_c\right)}\left[1-p+p\cos\left(4J_h\tau_h\right)\right]\sin\left(2J_c\tau_c\right)/Z_{R_c},\\
g_3 &= e^{-i\left(\varphi_s+\tau_c\omega_c+\tau_h\omega_h\right)}\cos\left(2J_c\tau_c\right)\cos\left(2J_h\tau_h\right),
\end{aligned}
\tag{A1}
$$

while that for equations (13)–(15) are

$$
\begin{aligned}
f_3' &= \frac{1}{2}ie^{-i\phi_h}\cos^2\left(2J_c\tau_c\right)\sin\left(4J_h\tau_h\right)/Z_{R_h},\\
g_1' &= ie^{i\left(\phi_h+\varphi_s-\tau_c\omega_c-\tau_h\omega_h\right)}\cos\left(2J_c\tau_c\right)\sin\left(2J_h\tau_h\right)/Z_{R_h},\\
g_2' &= e^{i\left(\varphi_s-\tau_c\omega_c-\tau_h\omega_h\right)}\cos\left(2J_c\tau_c\right)\sin\left(2J_h\tau_h\right).
\end{aligned}
\tag{A2}
$$

ORCID iD

Zhong-Xiao Man https://orcid.org/0000-0003-1906-5923

References

[1] Nielsen M and Chuang I 2000 *Quantum Computation and Quantum Information* (Cambridge University Press)
[2] Gemma G, Michel M and Mahler G 2004 *Quantum Thermodynamics* (Springer)
[3] Deffner S and Campbell S 2019 *Quantum Thermodynamics: An Introduction to the Thermodynamics of Quantum Information* (Morgan and Claypool Publishers) pp 2053–571
[4] Kosloff R 2013 Quantum thermodynamics: a dynamical viewpoint *Entropy* **15** 2100
[5] Vinjanampathy S and Anders J 2016 Quantum thermodynamics *Contemp. Phys.* **57** 545
[6] Goold J, Huber M, Riera A, del Rio L and Skrzypczyk P 2016 The role of quantum information in thermodynamics-a topical review *J. Phys. A: Math. Theor.* **49** 143001
[7] Millen J and Xuereb A 2016 Perspective on quantum thermodynamics *New J. Phys.* **18** 011002
[8] Brunner N, Huber M, Linden N, Popescu S, Silva R and Skrzypczyk P 2014 Entanglement enhances cooling in microscopic quantum refrigerators *Phys. Rev.* E **89** 032115
[9] Hewgill A, Ferraro A and De Chiara G 2018 Quantum correlations and thermodynamic performances of two-qubit engines with local and common baths *Phys. Rev.* A **98** 042102
[10] Feldmann T and Kosloff R 2012 Short time cycles of purely quantum refrigerators *Phys. Rev.* E **85** 051114
[11] Feldmann T and Kosloff R 2006 Quantum lubrication: suppression of friction in a first-principles four-stroke heat engine *Phys. Rev.* E **73** 025107
[12] Correa L A, Palao J P and Alonso D 2015 Internal dissipation and heat leaks in quantum thermodynamic cycles *Phys. Rev.* E **92** 032136
[13] Camati P A, Santos J F G and Serra R M 2019 Coherence effects in the performance of the quantum otto heat engine *Phys. Rev.* A **99** 062103
[14] Klatzow J, Becker J N, Ledingham P M, Weinzetl C, Kaczmarek K T, Saunders D J, Nunn J, Walmsley I A, Uzdin R and Poem E 2019 Experimental demonstration of quantum effects in the operation of microscopic heat engines *Phys. Rev. Lett.* **122** 110601
[15] Uzdin R, Levy A and Kosloff R 2015 Equivalence of quantum heat machines and quantum-thermodynamic signatures *Phys. Rev.* X **5** 031044
[16] Peterson J P S, Batalhão T B, Herrera M, Souza A M, Sarthour R S, Oliveira I S and Serra R M 2019 Experimental characterization of a spin quantum heat engine *Phys. Rev. Lett.* **123** 240601
[17] Zhang T, Liu W T, Chen P X and Li C Z 2007 Four-level entangled quantum heat engines *Phys. Rev.* A **75** 062102
[18] Barrios G A, Albarrán-Arriagada F, Cárdenas-López F A, Romero G and Retamal J C 2017 Role of quantum correlations in light-matter quantum heat engines *Phys. Rev.* A **96** 052119
[19] Dillenschneider R and Lutz E 2009 Energetics of quantum correlations *EPL* **88** 50003
[20] Park J J, Kim K-H, Sagawa T and Kim S W 2013 Heat engine driven by purely quantum information *Phys. Rev. Lett.* **111** 230402
[21] Brandner K, Bauer M, Schmid M T and Seifert U 2015 Coherence-enhanced efficiency of feedback-driven quantum engines *New J. Phys.* **17** 065006
[22] Rahav S, Harbola U and Mukamel S 2012 Heat fluctuations and coherences in a quantum heat engine *Phys. Rev.* A **86** 043843
[23] Uzdin R 2016 Coherence-induced reversibility and collective operation of quantum heat machines via coherence recycling *Phys. Rev. Appl.* **6** 024004
[24] Dorfman K E, Xu D and Cao J 2018 Efficiency at maximum power of a laser quantum heat engine enhanced by noise-induced coherence *Phys. Rev.* E **97** 042120
[25] Doyeux P, Leggio B, Messina R and Antezza M 2016 Quantum thermal machine acting on a many-body quantum system: role of correlations in thermodynamic tasks *Phys. Rev.* E **93** 022134

[26] Türkpençe D and Müstecaplıoğlu O E 2016 Quantum fuel with multilevel atomic coherence for ultrahigh specific work in a photonic carnot engine *Phys. Rev.* E **93** 012145
[27] Dağ C B, Niedenzu W, Müstecaplıoğlu O E and Kurizki G 2016 Multiatom quantum coherences in micromasers as fuel for thermal and nonthermal machines *Entropy* **18** 244
[28] Türkpençe D, Altintas F, Paternostro M and Müstecaplıoğlu O E 2017 A photonic carnot engine powered by a spin-star network *Europhys. Lett.* **117** 50002
[29] Hammam K, Leitch H, Hassouni Y and Chiara G D 2022 Exploiting coherence for quantum thermodynamic advantage *New J. Phys.* **24** 113053
[30] Hammam K, Hassouni Y, Fazio R and Manzano G 2021 Optimizing autonomous thermal machines powered by energetic coherence *New J. Phys.* **23** 043024
[31] Latune C L, Sinayskiy I and Petruccione F 2019 Quantum coherence, many-body correlations and non-thermal effects for autonomous thermal machines *Sci. Rep.* **9** 3191
[32] Niedenzu W, Gelbwaser-Klimovsky D, Kofman A G and Kurizki G 2016 On the operation of machines powered by quantum non-thermal baths *New J. Phys.* **18** 083012
[33] Yu W-L, Li T, Li H, Zhang Y, Zou J and Wang Y-D 2021 Heat modulation on target thermal bath via coherent auxiliary bath *Entropy* **23** 1183
[34] Ma Y-H, Liu C and Sun C 2021 Works with quantum resource of coherence (arXiv:2110.04550 [quant-ph])
[35] Guff T, Daryanoosh S, Baragiola B Q and Gilchrist A 2019 Power and efficiency of a thermal engine with a coherent bath *Phys. Rev.* E **100** 032129
[36] Li L, Zou J, Li H, Xu B-M, Wang Y-M and Shao B 2018 Effect of coherence of nonthermal reservoirs on heat transport in a microscopic collision model *Phys. Rev.* E **97** 022111
[37] Manatuly A, Niedenzu W, Román-Ancheyta R, Çakmak B, Müstecaplıoğlu O E and Kurizki G 2019 Collectively enhanced thermalization via multiqubit collisions *Phys. Rev.* E **99** 042145
[38] Román-Ancheyta R, Çakmak B and Müstecaplıoğlu O E 2019 Spectral signatures of non-thermal baths in quantum thermalization *Quantum Sci. Technol.* **5** 015003
[39] Rodrigues F L S, De Chiara G, Paternostro M and Landi G T 2019 Thermodynamics of weakly coherent collisional models *Phys. Rev. Lett.* **123** 140601
[40] De Chiara G and Antezza M 2020 Quantum machines powered by correlated baths *Phys. Rev. Res.* **2** 033315
[41] Scully M O, Zubairy M S, Agarwal G S and Walther H 2003 Extracting work from a single heat bath via vanishing quantum coherence *Science* **299** 862
[42] Zhang Q, Man Z-X, Zhang Y-J, Yan W-B and Xia Y-J 2023 Quantum thermodynamics in nonequilibrium reservoirs: Landauer-like bound and its implications *Phys. Rev.* A **107** 042202
[43] Latune C L, Sinayskiy I and Petruccione F 2019 Apparent temperature: demystifying the relation between quantum coherence, correlations and heat flows *Quantum Sci. Technol.* **4** 025005
[44] Santos J P, Céleri L C, Landi G T and Paternostro M 2019 The role of quantum coherence in non-equilibrium entropy production *npj Quantum Inf.* **5** 23
[45] Latune C L, Sinayskiy I and Petruccione F 2020 Negative contributions to entropy production induced by quantum coherences *Phys. Rev.* A **102** 042220
[46] Latune C L, Sinayskiy I and Petruccione F 2019 Heat flow reversals without reversing the arrow of time: the role of internal quantum coherences and correlations *Phys. Rev. Res.* **1** 033097
[47] Tajima H and Funo K 2021 Superconducting-like heat current: effective cancellation of current-dissipation trade-off by quantum coherence *Phys. Rev. Lett.* **127** 190604
[48] Çakmak B, Manatuly A and Müstecaplıoğlu O E 2017 Thermal production, protection and heat exchange of quantum coherences *Phys. Rev.* A **96** 032117
[49] Kaneyasu M and Hasegawa Y 2023 Quantum otto cycle under strong coupling *Phys. Rev.* E **107** 044127
[50] Mehta V and Johal R S 2017 Quantum otto engine with exchange coupling in the presence of level degeneracy *Phys. Rev.* E **96** 032110
[51] Purkait C and Biswas A 2023 Measurement-based quantum otto engine with a two-spin system coupled by anisotropic interaction: enhanced efficiency at finite times *Phys. Rev.* E **107** 054110
[52] Ishizaki M, Hatano N and Tajima H 2023 Switching the function of the quantum otto cycle in non-Markovian dynamics: heat engine, heater and heat pump *Phys. Rev. Res.* **5** 023066
[53] Cherubim C, de Oliveira T R and Jonathan D 2022 Nonadiabatic coupled-qubit otto cycle with bidirectional operation and efficiency gains *Phys. Rev.* E **105** 044120
[54] Son J, Talkner P and Thingna J 2021 Monitoring quantum otto engines *PRX Quantum* **2** 040328
[55] Singh V and Müstecaplıoğlu O E 2020 Performance bounds of nonadiabatic quantum harmonic otto engine and refrigerator under a squeezed thermal reservoir *Phys. Rev.* E **102** 062123
[56] Chen J-F, Sun C-P and Dong H 2019 Achieve higher efficiency at maximum power with finite-time quantum otto cycle *Phys. Rev.* E **100** 062140
[57] Leggio B and Antezza M 2016 Otto engine beyond its standard quantum limit *Phys. Rev.* E **93** 022122
[58] Rau J 1963 Relaxation phenomena in spin and harmonic oscillator systems *Phys. Rev.* **129** 1880
[59] Ciccarello F, Lorenzo S, Giovannetti V and Palma G M 2022 Quantum collision models: open system dynamics from repeated interactions *Phys. Rep.* **954** 1
[60] Cattaneo M, De Chiara G, Maniscalco S, Zambrini R and Giorgi G L 2021 Collision models can efficiently simulate any multipartite Markovian quantum dynamics *Phys. Rev. Lett.* **126** 130403
[61] Ziman M and Bužek V 2005 All (qubit) decoherences: complete characterization and physical implementation *Phys. Rev.* A **72** 022110
[62] Benenti G and Palma G M 2007 Reversible and irreversible dynamics of a qubit interacting with a small environment *Phys. Rev.* A **75** 052110
[63] Gennaro G, Benenti G and Palma G M 2009 Relaxation due to random collisions with a many-qudit environment *Phys. Rev.* A **79** 022105
[64] Campbell S and Vacchini B 2021 Collision models in open system dynamics: a versatile tool for deeper insights? *Europhys. Lett.* **133** 60001

[65] Man Z-X, Xia Y-J and Lo Franco R 2018 Temperature effects on quantum non-Markovianity via collision models *Phys. Rev.* A **97** 062104
[66] Jin J S and Yu C s 2018 Non-markovianity in the collision model with environmental block *New J. Phys.* **20** 053026
[67] Barra F 2015 The thermodynamic cost of driving quantum systems by their boundaries *Sci. Rep.* **5** 14873
[68] Chiara G D, Landi G, Hewgill A, Reid B, Ferraro A, Roncaglia A J and Antezza M 2018 Reconciliation of quantum local master equations with thermodynamics *New J. Phys.* **20** 113024
[69] Lorenzo S, McCloskey R, Ciccarello F, Paternostro M and Palma G M 2015 Landauer's principle in multipartite open quantum system dynamics *Phys. Rev. Lett.* **115** 120403
[70] Pezzutto M, Paternostro M and Omar Y 2016 Implications of non-Markovian quantum dynamics for the landauer bound *New J. Phys.* **18** 123018
[71] Man Z-X, Xia Y-J and Franco R L 2019 Validity of the landauer principle and quantum memory effects via collisional models *Phys. Rev.* A **99** 042106
[72] Seah S, Nimmrichter S, Grimmer D, Santos J P, Scarani V and Landi G T 2019 Collisional quantum thermometry *Phys. Rev. Lett.* **123** 180602
[73] Barra F 2019 Dissipative charging of a quantum battery *Phys. Rev. Lett.* **122** 210601
[74] Karevski D and Platini T 2009 Quantum nonequilibrium steady states induced by repeated interactions *Phys. Rev. Lett.* **102** 207207
[75] Cusumano S, Cavina V, Keck M, De Pasquale A and Giovannetti V 2018 Entropy production and asymptotic factorization via thermalization: a collisional model approach *Phys. Rev.* A **98** 032119
[76] Hewgill A, González J O, Palao J P, Alonso D, Ferraro A and De Chiara G 2020 Three-qubit refrigerator with two-body interactions *Phys. Rev.* E **101** 012109
[77] Hardal A U C, Paternostro M and Müstecaplıoğlu O E 2018 Phase-space interference in extensive and nonextensive quantum heat engines *Phys. Rev.* E **97** 042127
[78] Chand S, Dasgupta S and Biswas A 2021 Finite-time performance of a single-ion quantum otto engine *Phys. Rev.* E **103** 032144
[79] Abah O, Roßnagel J, Jacob G, Deffner S, Schmidt-Kaler F, Singer K and Lutz E 2012 Single-ion heat engine at maximum power *Phys. Rev. Lett.* **109** 203006
[80] Roßnagel J, Dawkins S T, Tolazzi K N, Abah O, Lutz E, Schmidt-Kaler F and Singer K 2016 A single-atom heat engine *Science* **352** 325
[81] Roßnagel J, Abah O, Schmidt-Kaler F, Singer K and Lutz E 2014 Nanoscale heat engine beyond the carnot limit *Phys. Rev. Lett.* **112** 030602